# Phycobilisome-Deficient Strains of *Synechocystis* sp. PCC 6803 Have Reduced Size and Require Carbon-Limiting Conditions to Exhibit Enhanced Productivity[1][W][OPEN]

**David J. Lea-Smith*, Paolo Bombelli, John S. Dennis, Stuart A. Scott, Alison G. Smith, and Christopher J. Howe**

Department of Biochemistry, University of Cambridge, Cambridge CB2 1QW, United Kingdom (D.J.L.-S., P.B., C.J.H.); Department of Chemical Engineering and Biotechnology, University of Cambridge, Cambridge CB2 3RA, United Kingdom (J.S.D.); Department of Engineering, University of Cambridge, Cambridge CB2 1PZ, United Kingdom (S.A.S.); and Department of Plant Sciences, University of Cambridge, Cambridge CB2 3EA, United Kingdom (A.G.S.)

Reducing excessive light harvesting in photosynthetic organisms may increase biomass yields by limiting photoinhibition and increasing light penetration in dense cultures. The cyanobacterium *Synechocystis* sp. PCC 6803 harvests light via the phycobilisome, which consists of an allophycocyanin core and six radiating rods, each with three phycocyanin (PC) discs. Via targeted gene disruption and alterations to the promoter region, three mutants with two ($p_{cpc}$T→C) and one (ΔCpcC1C2:$p_{cpc}$T→C) PC discs per rod or lacking PC (olive) were generated. Photoinhibition and chlorophyll levels decreased upon phycobilisome reduction, although greater penetration of white light was observed only in the PC-deficient mutant. In all strains cultured at high cell densities, most light was absorbed by the first 2 cm of the culture. Photosynthesis and respiration rates were also reduced in the ΔCpcC1C2:$p_{cpc}$T→C and olive mutants. Cell size was smaller in the $p_{cpc}$T→C and olive strains. Growth and biomass accumulation were similar between the wild-type and $p_{cpc}$T→C under a variety of conditions. Growth and biomass accumulation of the olive mutant were poorer in carbon-saturated cultures but improved in carbon-limited cultures at higher light intensities, as they did in the ΔCpcC1C2:$p_{cpc}$T→C mutant. This study shows that one PC disc per rod is sufficient for maximal light harvesting and biomass accumulation, except under conditions of high light and carbon limitation, and two or more are sufficient for maximal oxygen evolution. To our knowledge, this study is the first to measure light penetration in bulk cultures of cyanobacteria and offers important insights into photobioreactor design.

Cyanobacteria (oxygenic photosynthetic bacteria) are increasingly being considered for chemical and biomass production (Ducat et al., 2011) due to their highly efficient conversion of water and carbon dioxide ($CO_2$) to biomass using solar energy (Dismukes et al., 2008), growth on non-arable land with minimal nutrients, and the ease with which many species can be genetically manipulated. However, further improvements in efficiency are desirable for large-scale industrial production. Such gains could, in principle, be derived from reducing losses due to respiration or unproductive light harvesting, increasing carbon fixation rates by enhancing Rubisco catalysis and specificity for $CO_2$, and broadening the spectrum of light absorption (Blankenship et al., 2011). We recently demonstrated that reducing respiration in the model species *Synechocystis* sp. PCC 6803 resulted in slower growth under diurnal conditions (Lea-Smith et al., 2013). Improving Rubisco by genetic manipulation has proved difficult (Whitney et al., 2011), and due to the carbon-concentrating properties of the carboxysome, cyanobacterial Rubisco has the highest carboxylation velocity among photosynthetic organisms (Savir et al., 2010). Extending the spectral range of light absorption is challenging, since it requires either the incorporation of foreign pigments into photosystems or the introduction of novel light-harvesting complexes (Chen and Blankenship, 2011). Therefore, decreasing unproductive light harvesting may be the most promising approach.

Several studies have focused on this by reducing the antenna size in unicellular algae and cyanobacteria (Melis, 2009). These organisms have evolved to maximize light harvesting, a characteristic that may be advantageous for evolutionary success but is unfavorable for biomass production, especially in dense cell environments, such as in photobioreactors or raceway ponds. Under these conditions, cells in the upper layer will receive saturating light, absorbing more energy than can be

[1] This work was supported by Shell Global Solutions.

* Address correspondence to djl63@cam.ac.uk.

The author responsible for distribution of materials integral to the findings presented in this article in accordance with the policy described in the Instructions for Authors (www.plantphysiol.org) is: David J. Lea-Smith (djl63@cam.ac.uk).

[W] The online version of this article contains Web-only data.

[OPEN] Articles can be viewed online without a subscription.

www.plantphysiol.org/cgi/doi/10.1104/pp.114.237206

utilized by photosynthesis, with the excess being dissipated as heat or fluorescence. Net photosynthesis and biomass accumulation are reduced by photoinhibition, the direct damage of photosynthetic proteins by sunlight, and the production of reactive oxygen species, which further damages the photosynthetic machinery (Mussgnug et al., 2007; Beckmann et al., 2009; Ritchie and Larkum, 2012). Photosynthetic rates increase with the depth in the pond due to decreased photoinhibition until a maximum rate is achieved. Below this depth, the light intensity is insufficient for maximal photosynthesis and yields are reduced by respiration (Ritchie and Larkum, 2012). In theory, reducing the antenna should increase biomass accumulation by decreasing energy losses and photoinhibition at the surface while allowing additional light to penetrate to lower depths, thus maximizing the percentage of cells harvesting light.

Reduction of the light-harvesting complex in the green alga *Chlamydomonas reinhardtii* has been demonstrated to increase photosynthetic efficiency, reduce photoinhibition, and increase mid log phase growth under saturating light (Mussgnug et al., 2007; Beckmann et al., 2009). Similar studies have been performed in cyanobacteria (Nakajima and Ueda, 1997; Page et al., 2012; Kwon et al., 2013), which typically harvest light via a large cytosolic localized antenna complex, the phycobilisome (PBS). This associates with PSII and PSI, resulting in energy transfer to the reaction centers (Mullineaux et al., 1997). In *Synechocystis* sp. PCC 6803, the PBS comprises a core allophycocyanin (APC) region (wavelength of maximum light absorption [$\lambda_{max}$] = 652 nm) and six radiating rods, each composed of three stacked disc-shaped phycocyanin (PC) hexamers ($\lambda_{max}$ = 625 nm; Glazer, 1989; Arteni et al., 2009). The hexamers consist of alternating $\alpha$PC and $\beta$PC phycobiliproteins, encoded by *cpcA* (for phycocyanin alpha) and *cpcB* (for phycocyanin beta), respectively (Plank and Anderson, 1995). Linker proteins connect the discs; the disc proximal to the APC core is connected via CpcG1 or CpcG2 (Kondo et al., 2007), the middle disc via CpcC1, and the distal disc via CpcC2 (Ughy and Ajlani, 2004). Since the PBS is larger than both photosystems and absorbs light at different wavelengths from the chlorophylls and carotenoids in the reaction centers, it increases both the area and the spectral range of light harvested. A *Synechocystis* sp. PCC 6714 mutant with a T→C substitution 5 bp downstream of the transcription initiation site of the *cpcBAC1C2D* operon (PD-1; Imashimizu et al., 2003) and containing only one-third the level of PC (Nakajima et al., 1998) demonstrated reduced photoinhibition and 20% to 30% higher photosynthesis, as determined by higher oxygen evolution rates, in dense cultures under high light (Nakajima and Ueda, 1997). However, biomass accumulation and growth were not quantified in these studies. More recently, Page et al. (2012) quantified biomass accumulation and photosynthetic rates in three mutants of *Synechocystis* sp. PCC 6803: CB, containing only one PC hexamer per rod, a PC-deficient mutant (olive), and a mutant completely lacking PBSs. In contrast to the studies in *C. reinhardtii*, decreasing antenna size in *Synechocystis* sp. PCC 6803 resulted in lower biomass productivity. However, productivity was tested only in conical flasks and flat-panel bioreactors with a culture depth of approximately 2 cm. Under such low depths, any productivity benefits due to the effects of greater light penetration would not be observed (Ritchie and Larkum, 2012). The maximum light intensity utilized was 150 $\mu$mol photons $m^{-2}$ $s^{-1}$, which is significantly lower than full sunlight. Moreover, the CB mutant contains a large amount of free phycobiliproteins not associated with the PBS (Ughy and Ajlani, 2004; Collins et al., 2012). These absorb light and dissipate it as heat and fluorescence, which would further lower productivity. Another recent study showed that the olive mutant achieved higher cell densities than the wild type under 400 $\mu$mol photons $m^{-2}$ $s^{-1}$ light in 5-L flat-bed photobioreactors, although biomass accumulation was not measured (Kwon et al., 2013).

In this study, we generated three antenna-truncated mutants with decreasing amounts of PC in order to determine the optimal PBS size for maximal productivity in dense cultures and to understand further the role of this complex in cyanobacteria. We demonstrate that reducing the PBS lowered photoinhibition, but when cells were exposed to a white light-emitting diode (LED), light penetration increased only in the strain lacking any PC. Deletion of more than one PC disc per rod reduced photosynthesis and biomass yields, except under conditions of high light exposure and carbon limitation. This suggests that two to three PC discs per rod, commonly found in most cyanobacteria, is optimal for light harvesting in industrial processes.

## RESULTS

### Generation of Recombinant Strains of *Synechocystis* sp. PCC 6803

Unmarked mutants of *Synechocystis* sp. PCC 6803 with two PC hexamers per rod (ΔCpcC2), one PC hexamer per rod (ΔCpcC1C2), and no PC (olive) were constructed by disruption of *cpcC2*, *cpcC1C2*, and *cpcBAC1C2*, respectively, via a two-step homologous recombination protocol. Deletion of the entire PBS results in extremely poor growth (Ajlani and Vernotte, 1998; Page et al., 2012; Kwon et al., 2013), so this mutant was not generated. Plasmids in which the genes of interest were disrupted with a cassette encoding neomycin phosphotransferase/levansucrase (*npt1/sacRB*) were introduced into *Synechocystis* sp. PCC 6803, and transformants were selected in the presence of kanamycin. Following complete segregation of strains, markerless constructs containing deleted copies of the target genes and lacking the *npt1/sacRB* cassette were introduced, and cells were cultured in the presence of Suc to select for recombination-mediated removal of the cassette. Complete segregation was confirmed by PCR assays with primers upstream and downstream of the respective genes (Supplemental Fig. S1). Analysis of purified PBS preparations in Suc gradients confirmed the presence of free phycobiliproteins in the ΔCpcC2 and ΔCpcC1C2 strains (Fig. 1A), which is

consistent with previous studies (Ughy and Ajlani, 2004), and PC absorbance was similar to the wild type (Supplemental Fig. S2A). Loss of appropriate subunits in the PBS complex was confirmed via SDS-PAGE (Fig. 1B).

In order to remove free phycobiliproteins, we altered the strength of the *cpc* promoter. The T nucleotide that was altered to C in the *Synechocystis* sp. PCC 6714 PD mutant is conserved in *Synechocystis* sp. PCC 6803, 258 bp upstream of *cpcB* (position 727,723 in the *Synechocystis* sp. PCC 6803 genome; Supplemental Fig. S3). Therefore, the same nucleotide substitution and an additional T→G substitution, which has also been shown to lower transcription (Imashimizu et al., 2003), were introduced into the wild type and the ΔCpcC2 and ΔCpcC1C2 mutants via two-step homologous recombination. The promoter region around the T nucleotide was first replaced with an *npt1/sacRB* cassette. Following complete segregation of strains, markerless constructs containing the promoter region with the appropriate nucleotide substitution were introduced and Suc-resistant colonies were selected. Introduction of the desired nucleotide substitution was confirmed by sequencing. Only the T→C substitution resulted in the complete removal of free phycobiliproteins (Fig. 1A). The $p_{cpc}$T→C and ΔCpcC2:$p_{cpc}$T→C strains demonstrated similar PBS profiles (Fig. 1B) and absorbance (Supplemental Fig. S2B), so only the first strain was used for further study. In addition to this strain, the ΔCpcC1C2:$p_{cpc}$T→C strain, which contains only one PC disc per rod

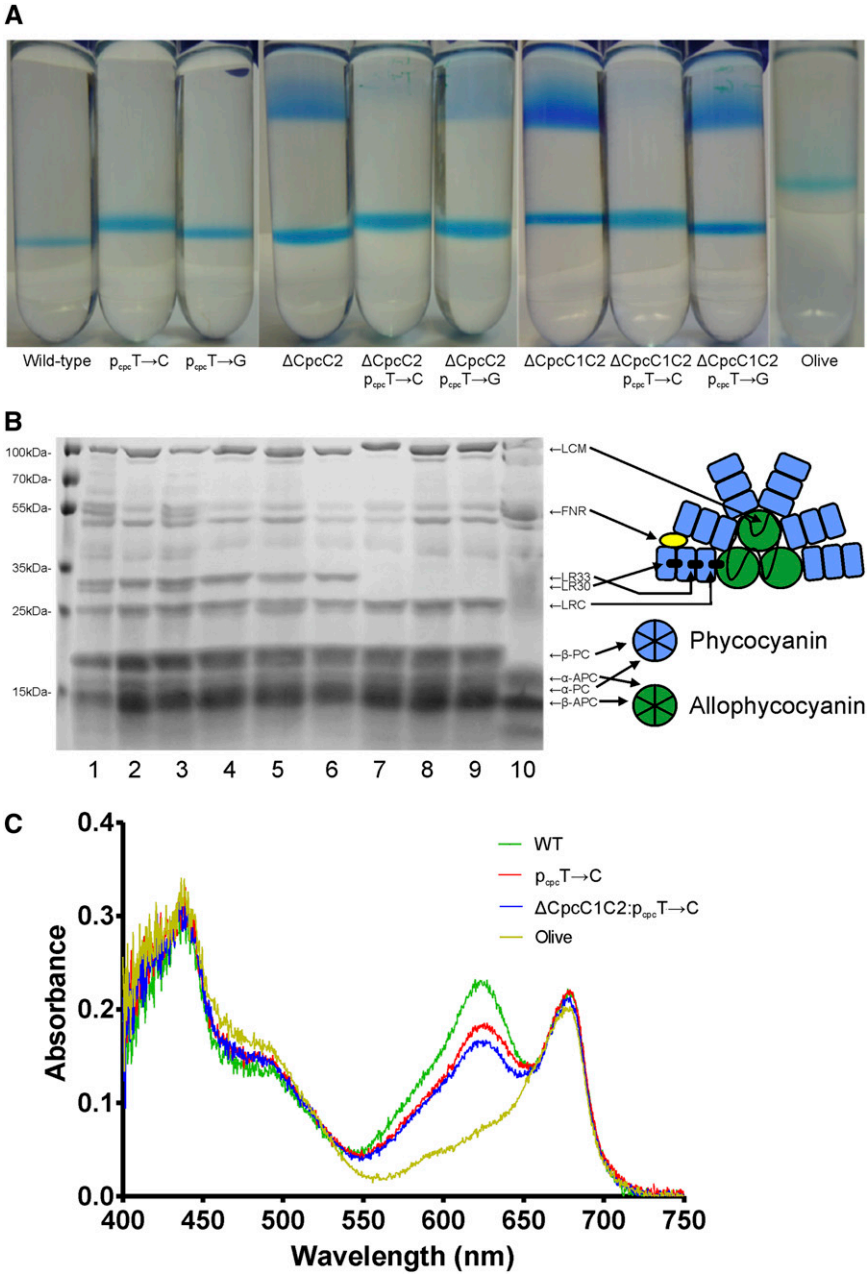


**Figure 1.** Analysis of attenuated PBS mutants. A and B, Suc gradients of purified PBSs (A) and separation of PBS polypeptides by Tris-HCl polyacrylamide gradient gel electrophoresis (B) from the wild type (lane 1), $p_{cpc}$T→C (lane 2), $p_{cpc}$T→G (lane 3), ΔCpcC2 (lane 4), ΔCpcC2:$p_{cpc}$T→C (lane 5), ΔCpcC2:$p_{cpc}$T→G (lane 6), ΔCpcC1C2 (lane 7), ΔCpcC1C2:$p_{cpc}$T→C (lane 8), ΔCpcC1C2:$p_{cpc}$T→G (lane 9), and ΔCpcBAC1C2 (lane 10). In A, the bottom band in all samples corresponds to intact PBS. The top blue band in lanes 4, 6, 7, and 9 consists of free phycobiliproteins (Ughy and Ajlani, 2004). Migration of the PBS band is dependent on size; larger complexes are lower in the column. In B, the identity of specific polypeptides is indicated in the schematic representation of the PBS of *Synechocystis* sp. PCC 6803 (Glazer, 1988). C, Spectrum showing the absorbance of the four strains used in subsequent studies. Values are averages from four biological replicates and are standardized to 750 nm. WT, Wild type.

(Fig. 1B) and reduced PC absorbance (Fig. 1C), and the olive mutant were selected for characterization.

### Characterization of Attenuated PBS Mutants

To test for photoinhibition, all strains were grown under continuous moderate white light (40 $\mu$mol photons $m^{-2}$ $s^{-1}$) to mid log phase followed by incubation in the dark for 10 min. Cells were then incubated under constant saturating light at 2,000 $\mu$mol photons $m^{-2}$ $s^{-1}$ for 80 min in the absence and presence of lincomycin, during which time oxygen evolution was measured. Photoinhibition, as determined by a decrease in oxygen evolution, was similar between the wild-type and $p_{cpc}$T→C strains, the rate of oxygen evolution decreasing to 55.9% ± 4.9% and 52.3% ± 6.9% of the initial values, respectively (Fig. 2A). However, photoinhibition was significantly reduced in the ΔCpcC1C2:$p_{cpc}$T→C strain and further still in the olive mutant, with oxygen evolution decreasing to 78.45% ± 4.2% and 90.85% ± 14.5% of the initial rate. Oxygen evolution increased in the olive mutant for the first 20 min of light exposure, suggesting that 2,000 $\mu$mol photons $m^{-2}$ $s^{-1}$ is not saturating light for this strain, due to its decreased light absorption properties. A similar pattern was observed when strains were incubated in the presence of lincomycin, which inhibits protein synthesis and thus repair of PSII, except the $p_{cpc}$T→C strain, which showed greater photoinhibition than the wild type (Fig. 2B).

Photosynthetic rates were measured at different light intensities in order to generate a light saturation curve. In such curves, the rate of oxygen evolution levels off as saturating light intensity is approached, with the maximum rate of oxygen evolution designated as $P_{max}$. The $P_{max}$ of the olive and ΔCpcC1C2:$p_{cpc}$T→C mutants were 41% and 21%, respectively, lower than that of the wild type (Fig. 2C). By contrast, the $P_{max}$ for the $p_{cpc}$T→C mutant was marginally higher (7%), but not significantly different, from that of the wild type. The gradient of the oxygen evolution curve when the rate of oxygen evolution increases linearly in proportion to the light intensity (i.e. under nonsaturating light conditions) provides a measure of the photon yield (Φp; Melis, 2009). The wild type and the $p_{cpc}$T→C mutant showed similar Φp of 0.197 ± 0.015 and 0.199 ± 0.015, respectively. By contrast, the ΔCpcC1C2:$p_{cpc}$T→C and olive mutants demonstrated significantly lower Φp of 0.131 ± 0.010 and 0.117 ± 0.015, respectively. The rate of oxygen depletion in the dark after a period of illumination (i.e. cellular respiration) can also be plotted as a function of the light intensity prior to the dark period, giving the respiration curve (Fig. 2D). The maximum rate of oxygen depletion was measured after the highest light intensity. $p_{cpc}$T→C, ΔCpcC1C2:$p_{cpc}$T→C, and olive mutants showed 11%, 43%, and 60% decreases in maximum rate of oxygen depletion compared with the wild type. Superimposing the light saturation and respiration curves and extrapolating the linear regions to the point at which they intersect gives the light intensity

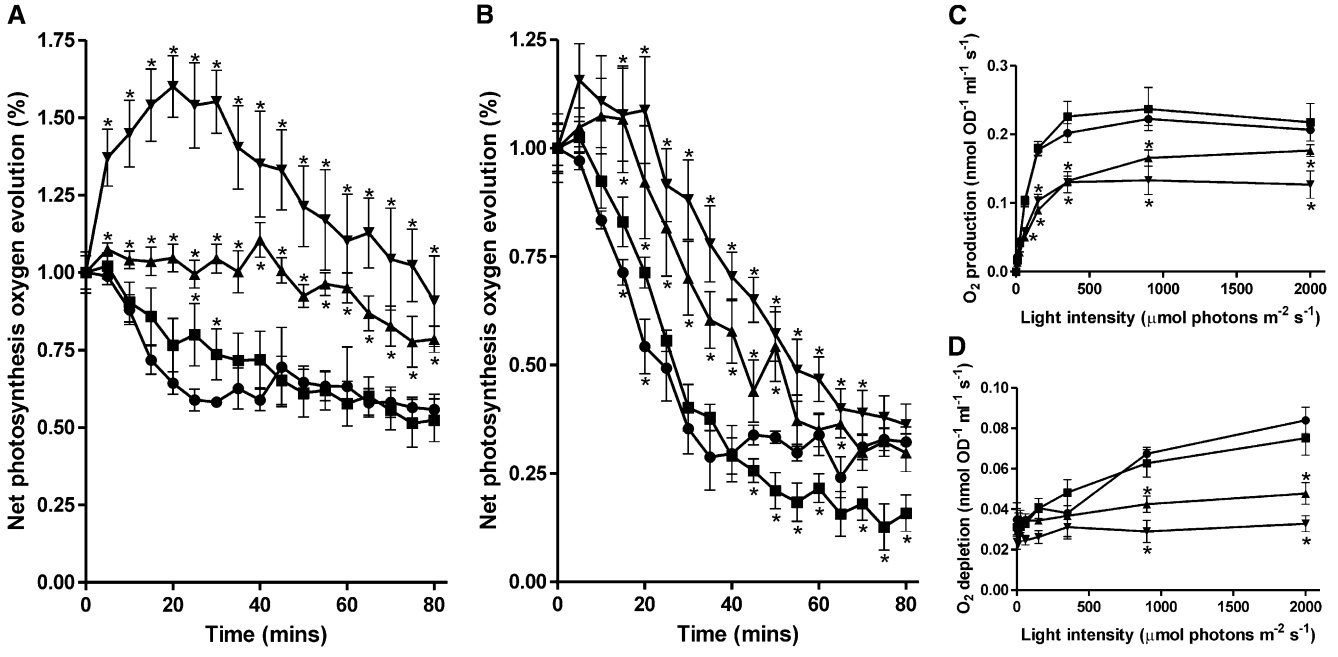


**Figure 2.** Characterization of wild-type (circles), $p_{cpc}$T→C (squares), ΔCpcC1C2:$p_{cpc}$T→C (up triangles), and olive (down triangles) strains. A and B, Photosynthetic oxygen evolution was measured in the absence (A) and presence (B) of lincomycin as a measure of photoinhibition. Light was at an intensity of 2,000 $\mu$mol photons $m^{-2}$ $s^{-1}$. C and D, Oxygen evolution was measured at different light intensities (C), and oxygen consumption was measured following each light period (D). All results are from four separate biological replicates. Errors bars indicate SD. Asterisks indicate significant differences between samples ($P < 0.05$).

required to reach the compensation point, where the rate of oxygen evolution and depletion compensate each other. Similar compensation point values (18.3 ± 1.4 and 18.7 ± 1.6 μmol photons $m^{-2}$ $s^{-1}$) were obtained for the wild type and the $p_{cpc}$T→C mutant, respectively. By contrast, significantly higher values, 39.5 ± 2.8 and 32.6 ± 5.9 μmol photons $m^{-2}$ $s^{-1}$, respectively, were obtained for the ΔCpcC1C2:$p_{cpc}$T→C and olive mutants.

Cell size was measured for each of the strains. The $p_{cpc}$T→C and olive mutants demonstrated successive reductions in size and cell volume compared with the wild type (Table I). All the PBS-truncated mutants demonstrated significant but similar reductions in chlorophyll per cell compared with the wild type (Table I).

### Light Penetration

Light penetration for cultures of the different strains at five different optical densities (O.D. 0.1, 0.5, 1, 2.5, and 5) and three light intensities (500, 1,000, and 2,000 μmol photons $m^{-2}$ $s^{-1}$) was measured at various depths using a quantum sensor (Fig. 3; Supplemental Fig. S4; Supplemental Table S1). Light penetration was also tested at three different wavelengths, red ($\lambda_{max}$ = 625 nm), green ($\lambda_{max}$ = 525 nm), and blue ($\lambda_{max}$ = 470 nm), at an intensity of 1,000 μmol photons $m^{-2}$ $s^{-1}$ in O.D. 1 cultures (Fig. 3; Supplemental Fig. S4, P–R). The data for light penetration can be characterized by calculating the attenuation coefficient ($\mu$), the rate at which light penetration decreases with depth. Under blue light, penetration was similar between all strains (Supplemental Table S1). Under red light and to a lesser extent under green light, penetration increased with the reduction of the antenna (Supplemental Table S1). The $\mu$ for the wild type, $p_{cpc}$T→C, ΔCpcC1C2:$p_{cpc}$T→C, and olive exposed to red light was 135.3, 105.2, 95.3, and 80.4 $m^{-1}$, respectively, and that for the same strains exposed to green light was 88.7, 87.1, 82.3, and 80.7 $m^{-1}$, respectively. However, under white light, the $\mu$ of wild-type cells was similar to that of mutants containing PC. For all cultures, the $\mu$ increased with O.D. ($\mu$ at O.D. 0.1 < $\mu$ at O.D. 0.5 < $\mu$ at O.D. 1 < $\mu$ at O.D. 2.5 < $\mu$ at O.D. 5), as expected. Under white light, a consistent difference was observed only between the wild type and the PC-less olive mutant, with the most dramatic difference at O.D. 2.5 (Fig. 3D; Supplemental Fig. S4). Under these conditions, the $\mu$ for the olive mutant was 24% smaller than that for the wild type (91.6 versus 120.3).

### Growth of PBS-Attenuated Mutants

In order to evaluate whether PBS reduction results in increases in growth and biomass accumulation, *Synechocystis* sp. PCC 6803 strains were cultured at different light intensities: 40 and 150 μmol photons $m^{-2}$ $s^{-1}$ in conical flasks with a culture depth of 2 cm, and 500 and 1,000 μmol photons $m^{-2}$ $s^{-1}$ in 250-mL containers with a culture depth of 10 cm, which may better reflect the depth in open ponds. Growth was measured by recording the O.D. and dry cell weight. When cultures were air bubbled, the olive mutant showed significantly slower growth at 40, 150, and 500 μmol photons $m^{-2}$ $s^{-1}$ (Fig. 4A; Supplemental Fig. S5, A and B) but improved growth at 1,000 μmol photons $m^{-2}$ $s^{-1}$ (Fig. 4B). The ΔCpcC1C2:$p_{cpc}$T→C mutant showed slower growth at 150 μmol photons $m^{-2}$ $s^{-1}$ but improved growth at 1,000 μmol photons $m^{-2}$ $s^{-1}$, although not as high as the olive mutant. Growth was similar between the wild-type and $p_{cpc}$T→C strains at all light intensities. No evidence of photobleaching was observed at 150 μmol photons $m^{-2}$ $s^{-1}$ (Supplemental Fig. S6B). Some photobleaching was observed at 500 μmol photons $m^{-2}$ $s^{-1}$ (Supplemental Fig. S6C), which increased at 1,000 μmol photons $m^{-2}$ $s^{-1}$ (Supplemental Fig. S6D). The PBS was not significantly altered over the time of the experiment, as determined by the ratio of APC to PC, at any light intensity (Supplemental Fig. S6, A–D). In order to determine whether biomass accumulation was different between the strains, the dry cell weight was measured at the end of each growth period in the cultures grown in the 250-mL containers. All strains accumulated similar biomass at 500 μmol photons $m^{-2}$ $s^{-1}$ (Fig. 4E), but the ΔCpcC1C2:$p_{cpc}$T→C and olive mutants accumulated significantly higher amounts at 1,000 μmol photons $m^{-2}$ $s^{-1}$, which correlated with the growth measurements (Fig. 4F).

Strains were then cultured in 250-mL containers and sparged with 5% $CO_2$ at 500 and 1,000 μmol photons $m^{-2}$ $s^{-1}$. Growth was similar between the PC-containing

**Table I.** *Cell size and chlorophyll content of strains*

Numbers of cells per unit of volume in cellular suspension at O.D. (750 nm) = 0.5 were measured by counting the cells directly using a Beckman Coulter 2Z particle counter. Cell diameter was directly measured using the same instrument. Cell volume was calculated from these measurements. Chlorophyll content was derived from the 750- and 680-nm values as described in "Materials and Methods." Results are from four biological replicates. SD is indicated. Asterisks indicate significant differences between samples ($P < 0.05$).

| Strain | Cells per 1 mL of Culture at O.D. (750 nm) = 1 ($10^6$ Cells) | Cell Diameter | Cell Volume | Chlorophyll Content | Chlorophyll Content per Cellular Volume |
|---|---|---|---|---|---|
| | | μm | $\mu m^3$ | amol $cell^{-1}$ | amol $\mu m^{-3}$ |
| Wild type | 145.2 ± 5.6 | 2.02 ± 0.05 | 4.34 ± 0.32 | 42.1 ± 2.6 | 9.69 ± 0.20 |
| $p_{cpc}$T→C | 192.5 ± 13.9* | 1.91 ± 0.04* | 3.66 ± 0.25* | 30.5 ± 1.1* | 8.35 ± 0.51* |
| ΔCpcC1C2:$p_{cpc}$T→C | 139.7 ± 7.2 | 1.99 ± 0.02 | 4.11 ± 0.13 | 35.0 ± 1.3* | 8.52 ± 0.17* |
| Olive | 224.8 ± 4.5* | 1.82 ± 0.01* | 3.17 ± 0.06* | 26.4 ± 0.6* | 8.33 ± 0.19* |

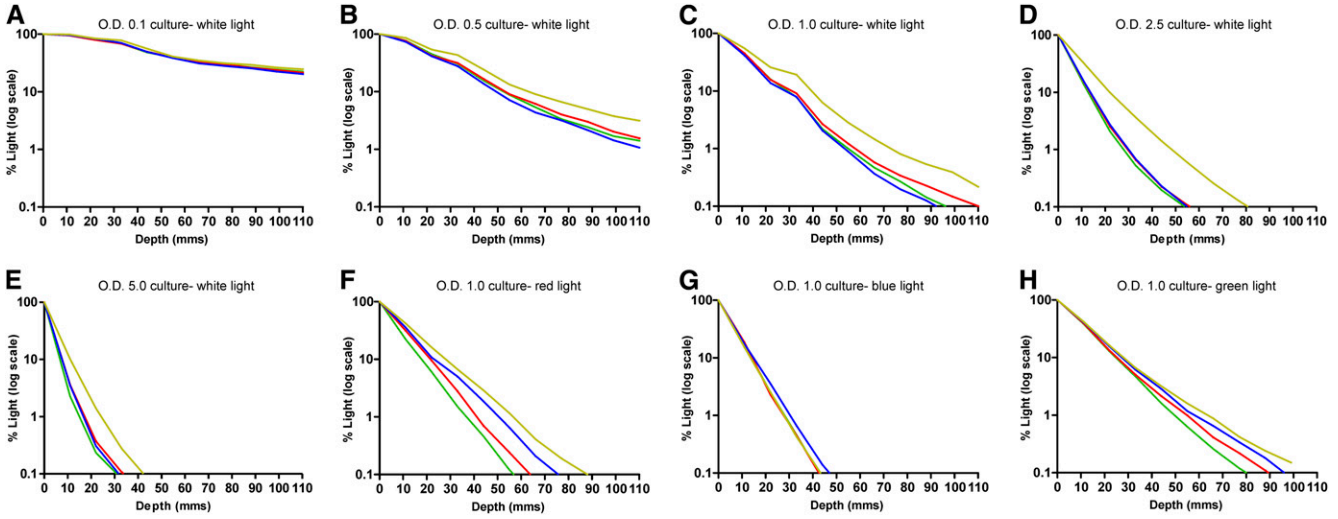


**Figure 3.** Light penetration as a function of the depth of wild-type (circles), $p_{cpc}$T→C (squares), ΔCpcC1C2:$p_{cpc}$T→C (up triangles), and olive (down triangles) strains. A to E, O.D. (750 nm) 0.1 (A), 0.5 (B), 1 (C), 2.5 (D), and 5 (E) cultures were exposed to 500, 1,000, or 2,000 $\mu$mol photons $m^{-2}$ $s^{-1}$, and light levels were measured at 11-mm intervals up to 110 mm. Results from these experiments are combined, as light penetration is independent of incident light intensity to at least 2,000 $\mu$mol photons $m^{-2}$ $s^{-1}$. F to H, O.D. (750 nm) 1 cultures were exposed to 1,000 $\mu$mol photons $m^{-2}$ $s^{-1}$ red (F), blue (G), and green (H) light, and light levels were measured at 11-mm intervals up to 99 mm. Light is expressed as a percentage in log scale. Results for separate light experiments are shown in Supplemental Figure S4.

strains but slower in the olive mutant (Fig. 4, C and D). Little if any photobleaching was observed, and the PBS was not significantly altered (Supplemental Fig. S6, E and F). Biomass accumulation was similar between all strains at 500 $\mu$mol photons $m^{-2}$ $s^{-1}$ but lower in the olive mutant at 1,000 $\mu$mol photons $m^{-2}$ $s^{-1}$ (Fig. 4, G and H). In all strains, biomass accumulation was higher in cultures sparged with 5% $CO_2$ than with air.

### Conservation of PBSs in Cyanobacteria

In order to determine the distribution of core and linker polypeptides in PBSs in cyanobacteria, a comparison of 86 sequenced strains was performed (Supplemental Table S2). Fourteen strains, including the PSII-deficient cyanobacterium strain UCYN-A (Zehr et al., 2008) and all the *Prochlorococcus* species, do not encode any of these PBS subunits, although

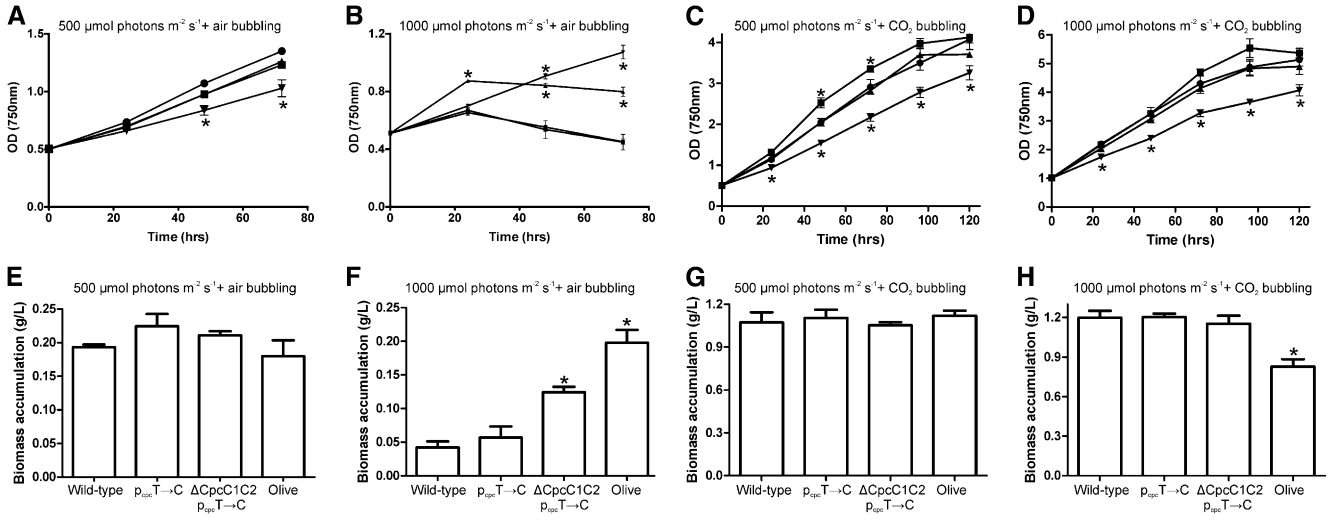


**Figure 4.** Growth (top) and biomass accumulation (bottom) of wild-type (circles), $p_{cpc}$T→C (squares), ΔCpcC1C2:$p_{cpc}$T→C (up triangles), and olive (down triangles) strains under different light and bubbling conditions. Strains were cultured at 500 (A and E) and 1,000 (B and F) $\mu$mol photons $m^{-2}$ $s^{-1}$ with air bubbling and at 500 (C and G) and 1,000 (D and H) $\mu$mol photons $m^{-2}$ $s^{-1}$ with 5% $CO_2$ bubbling. Results are from three to six biological replicates. Errors bars indicate SD. Asterisks indicate significant differences between samples ($P < 0.05$).

some species contain genes demonstrating high sequence similarity to those encoding phycoerthyrin subunits (Ting et al., 2001). Of the remaining strains, all encode homologs to *cpcG1*. Of these, 25 encode homologs only to *cpcC1*, 36 encode homologs to *cpcC1* and *cpcC2*, while the remaining 11 encode homologs to *cpcC1* and more than one *cpcC2* homolog.

## DISCUSSION

We have characterized a range of PBS-attenuated mutants under different growth conditions. As hypothesized, reducing the PBS generally resulted in lower photoinhibition, although this was not the case in the $p_{cpc}$T→C strain. In carbon-limited cultures, reduction of the PBS was clearly advantageous when strains were grown at 1,000 $\mu$mol photons $m^{-2}$ $s^{-1}$ (Fig. 4, B and F). The improved growth (Fig. 4B) and reduced photobleaching (Supplemental Fig. S6D) observed in the ΔCpcC1C2:$p_{cpc}$T→C and olive mutant strains under these conditions may also be due to lower photosynthetic rates, as demonstrated by the reduced rate of oxygen evolution (Fig. 2C). This would limit electron production overtaking consumption by the Calvin cycle, resulting in the photosynthetic electron transfer chain becoming less reduced. Under conditions where carbon is not limited, little photobleaching was observed, even at 1,000 $\mu$mol photons $m^{-2}$ $s^{-1}$ (Supplemental Fig. S6, E and F). In addition, cyanobacterial cultures sparged with $CO_2$ showed significantly higher growth rates and biomass accumulation than those sparged with air (Fig. 4, C and D and G and H compared with A and B and E and F, respectively). Although light penetration in cell suspensions increased as the PBS was gradually attenuated when red light and, to a lesser extent, green light, which is directly absorbed by PBSs, was used (Supplemental Fig. S4, P and R), reducing the PBS did not significantly improve overall light penetration when culture suspensions were exposed to white LED light, except in the PC-deficient strain (Fig. 3; Supplemental Fig. S4). This may reflect the fact that the red and green wavelengths are only a component of the spectrum (Supplemental Fig. S7) and/or that light scattering and absorption by other cellular components limit penetration to lower depths, suggesting that even one PC disc is sufficient to absorb enough light to give the same biomass production as the wild type. To the best of our knowledge, this study is the first to examine light penetration in any cyanobacterial cell suspension at different cell densities and light intensities. These experiments demonstrate that, in dense cultures (O.D. $\geq$ 2.5), the majority of light (80%–90%) is absorbed by cells in the top 1 to 2 cm of the culture.

Our results were similar to those observed by Page et al. (2012) when cultures were grown at low light intensity (40 $\mu$mol photons $m^{-2}$ $s^{-1}$ in our study [Supplemental Fig. S5A] and 50 $\mu$mol photons $m^{-2}$ $s^{-1}$ in Page et al., 2012) in conical flasks with air bubbling. Under these conditions, the olive mutant demonstrated lower biomass productivity than the wild type. Other results derived from our study are not comparable with those of Page et al. (2012), since the maximum light intensity used in their study was 150 $\mu$mol photons $m^{-2}$ $s^{-1}$. In another study (Kwon et al., 2013), the authors demonstrated 26% higher photosynthetic activity per cell in the olive mutant compared with the wild type, as measured by maximum oxygen evolution, at 400 $\mu$mol photons $m^{-2}$ $s^{-1}$ in continuous culture maintained at O.D. (680 nm) = 0.7. Whether this translates to greater productivity was not determined either by measuring biomass accumulation or cell density at O.D. (750 nm). In addition, measuring absorbance at O.D. (680 nm) quantifies both chlorophyll and cell density, which, given that chlorophyll content differs between strains (Table I), makes drawing any conclusion about productivity difficult. Therefore, drawing any reliable comparison between our results and those of Kwon et al. (2013) is not possible. However, the olive mutant may be useful for applications that require higher photosynthetic capacity, such as the generation of hydrogen (McCormick et al., 2013) or electricity in a biophotovoltaic device (Bombelli et al., 2011; Bradley et al., 2013).

The poorer performance of the olive mutant under most conditions is likely to be due to its significantly reduced photosynthetic capacity. This may be explained in part by a recent study by Collins et al. (2012) that examined membrane morphology and PSI and PSII distribution and amounts in PBS-truncated mutants. Significant morphological differences were observed in the olive mutant. In contrast to the wild type and the ΔCpcC1C2 mutant, where thylakoid membranes localized to the periphery of the cell in alignment with the cytoplasmic membrane, in the olive mutant, the membranes spanned the interior of the cell and appeared less curved. In both the olive and ΔCpcC1C2 mutants, the distance between thylakoid membranes was reduced from 40 to 32 nm. The PSI-PSII ratio was not significantly different in the ΔCpcC1C2 strain, but a reduction in the ratio of PSI to PSII was observed in the olive mutant, as was greater segregation and distance between the two photosystems. Despite the difference in the PSI-PSII ratio, the olive mutant has been shown to undergo state transitions (Bernát et al., 2009). Our study extended this work by examining cell size, chlorophyll levels, and photosynthetic and respiratory rates in these strains. The olive mutant cells are significantly smaller than wild-type cells (3.17 $\pm$ 0.06 versus 4.34 $\pm$ 0.32 $\mu m^3$; Table I), suggesting that this large complex, 5 to 10 MD, has a major effect on increasing cell size. The reduction in chlorophyll per cell in all PBS-attenuated mutants suggests that the total amount of PSII and/or PSI is lower (Table I). The decline in photosynthetic and respiratory capacity we observed may be due to the differences in membrane morphology.

The important role of the PBS in membrane organization, as illustrated by Collins et al. (2012), demonstrates the different roles this complex plays in the cell. However, under environmental conditions when strains are exposed to long periods of high light, having a smaller PBS, or no PBS at all, may be advantageous. *Prochlorococcus* spp., typically found in equatorial open ocean regions and potentially exposed to long periods of high light,

lack PBSs completely (Supplemental Table S2), although these species do contain homologs of *isiA*, encoding an iron stress-induced antenna complex (Bibby et al., 2001; Boekema et al., 2001). Lacking a PBS may also be critical in maintaining the small size of *Prochlorococcus* species, typically 0.5 to 0.7 $\mu$m in diameter, which is advantageous for nutrient uptake (Partensky et al., 1999). In strains containing PBSs, having one PC disc per rod is sufficient for maximal light harvesting and biomass accumulation, at least when $CO_2$ is not limiting. However, having at least two PC discs per rod is sufficient for maximal photosynthetic and respiratory activity, as indicated by the lower oxygen evolution and depletion rates in the ΔCpcC1C2:$p_{cpc}$T→C and olive mutant strains. This may explain why all PBS-containing cyanobacteria encode CpcC1 and, therefore, have at least two PC discs per rod (Supplemental Table S2).

## CONCLUSION

This study demonstrates that reducing the PBS is not useful for improving the industrial production of either cyanobacterial biomass or metabolites, except when carbon is limited, in contrast to the studies performed in *C. reinhardtii*. Lower photosynthetic activity has a detrimental effect on growth and is not compensated for by either reduced photoinhibition or greater light penetration. Photoinhibition may be further limited by mixing, which, in a culture where the majority of light penetrates only a few centimeters (Fig. 3; Supplemental Fig. S4), most likely limits the exposure of cells to light for brief periods. Given that light penetrates very poorly in dense cultures, our results suggest that metabolite production over an extended period of time may be optimal in flat-panel bioreactors or tubular bioreactors with thin diameters. While reduction of the PBS does not improve growth, a possible alternative might involve the development of PBSs containing at least two discs with pigments other than PC, such as phycoerythrin, which absorbs light at $\lambda_{max}$ = 545 nm, the part of the spectrum where light absorption by *Synechocystis* sp. PCC 6803 is lowest. Incorporation of phycoerythrobilins into PBSs was demonstrated in *Synechococcus* sp. PCC 7002 via the overexpression of *pebAB* (for 15,16-dihydrobiliverdin:ferredoxin oxidoreductase and phycoerythrobilin:ferredoxin oxidoreductase, respectively), encoding the two enzymes synthesizing this chromophore (Alvey et al., 2011). However, the overexpressing lines quickly reverted back to the wild-type PBS state. Stable incorporation of these pigments into PBSs may result in broader but lower absorption across the whole spectrum, increased light penetration, no difference in membrane morphology, and overall improved growth.

## MATERIALS AND METHODS

### Bacterial Strains, Media, and Growth Conditions

*Synechocystis* sp. PCC 6803 and strains derived from it were routinely cultured in BG-11 medium, supplemented with 10 mM sodium bicarbonate (Castenholz, 1988) at 30°C under moderate light (40 $\mu$mol photons $m^{-2}$ $s^{-1}$), and shaken at 160 rpm unless indicated otherwise. A total of 15 g $L^{-1}$ agar was used for the preparation of solid media, supplemented with 30 $\mu$g $mL^{-1}$ kanamycin and 5% (w/v) Suc when necessary. Strains used in this study are listed in Supplemental Table S3.

### Plasmid Construction

Primers used in this study are listed in Supplemental Table S4. PCR was performed by standard procedures using Phusion high-fidelity DNA polymerase (New England Biolabs). The genome sequence of *Synechocystis* sp. PCC 6803 (Kaneko et al., 1996) was consulted via Cyanobase (http://genome.kazusa.or.jp/cyanobase) for primer design. Gene deletion of *cpcC2* was performed by amplifying a 1,047-bp fragment upstream of *cpcC2* using primers CpcC2leftfor and CpcC2leftrev and a 1,089-bp fragment downstream of *cpcC2* using primers CpcC2rightfor and CpcC2rightrev, followed by insertion of the respective fragments into the *Xba*I/*Bam*HI and *Sac*I/*Eco*RI sites of pUC19 to generate pCpcC2-1. Gene deletion of *cpcC1C2* was performed by amplifying a 1,012-bp fragment upstream of *cpcC1* using primers CpcC1leftfor and CpcC1leftrev, followed by insertion of this fragment and the *cpcC2* downstream fragment into the *Xba*I/*Bam*HI and *Sac*I/*Eco*RI sites of pUC19 to generate pCpcC1C2-1. Gene deletion of *cpcBAC1C2* was performed by amplifying a 1,016-bp fragment downstream of *cpcB* using primers CpcBrightfor and CpcBrightrev, followed by insertion of this fragment and the *cpcC1* upstream fragment into the *Sac*I/*Eco*RI and *Xba*I/*Bam*HI sites of pUC19 to generate pCpcBAC1C2-1. The *Bam*HI-digested *npt1*/*sacRB* cassette from pUM24Cm (Ried and Collmer, 1987) was inserted into the *Bam*HI site between the upstream and downstream fragments in pCpcC2-1, pCpcC1C2-1, and pCpcBAC1C2-1 to generate pCpcC2-2, pCpcC1C2-2, and pCpcBAC1C2-2, respectively. Nucleotide substitution in the *cpc* operon promoter first required the generation of a marked mutant. This was performed by amplifying a 944-bp fragment upstream of the promoter region using primers Cpcproleftfor and Cpcproleftrev and a 1,018-bp fragment downstream of the promoter region using primers Cpcprorightfor and Cpcprorightrev, followed by insertion of the respective fragments into the *Eco*RI/*Bam*HI and *Bam*HI/*Hin*dIII sites of pUC19 to generate pCpcpro-1. The *Bam*HI-digested *npt1*/*sacRB* cassette was inserted into the *Bam*HI site between the upstream and downstream fragments in pCpcpro-1 to generate pCpcpro-2. A 635-bp fragment spanning the deleted region was then amplified using primers Cpcprointfor and Cpcprointrev, followed by insertion into the *Sma*I/*Hin*dIII sites of pUC19 to generate pCpcproint. Two fragments were then amplified with primers CpcprointforT-C and CpcprointforT-G, containing T→C and T→G substitutions, respectively, and the Cpcprointrev primer to generate 505-bp products. These fragments were cloned into the *Hin*cII/*Hin*dIII sites of pCpcproint. A *Sma*I/*Noc*I fragment was excised and inserted into the same sites in pCpcpro-1 to generate pCpcproT→C and pCpcproT→G. These plasmids contained the entire wild-type *cpc* promoter region, except for the T→C or T→G substitution 258 bp upstream of the *cpcB* start codon.

### Construction of PBS Mutant Strains

To generate marked mutants, approximately 1 $\mu$g of plasmids pCpcC2-2, pCpcC1C2-2, and pCpcBAC1C2-2 was mixed with *Synechocystis* sp. PCC 6803 cells for 6 h in liquid medium, followed by incubation on BG11 agar plates for approximately 24 h. An additional 3 mL of agar containing kanamycin was added to the surface of the plate followed by further incubation for approximately 1 to 2 weeks. Transformants were subcultured to allow the segregation of mutant alleles. Segregation was confirmed by PCR using primers CpcC2for/CpcC2rev, CpcC1for/CpcC2rev, or CpcC1for/CpcBrev, which flank the deleted region. Generation of unmarked mutants was carried out according to Xu et al. (2004). To remove the *npt1*/*sacRB* cassette, mutant lines were transformed with 1 $\mu$g of the markerless pCpcC2-1, pCpcC1C2-1, and pCpcBAC1C2-1 constructs. Following incubation in BG-11 liquid medium for 4 d and agar plates containing Suc for a further 1 to 2 weeks, transformants were patched on kanamycin and Suc plates. Suc-resistant, kanamycin-sensitive strains containing the unmarked deletion were confirmed by PCR using primers flanking the deleted region (Supplemental Fig. S1).

Wild-type, *cpcC2*, and *cpcC1C2* knockout lines with promoters containing the T→C or T→G substitution were generated by transformation with 1 $\mu$g of pCpcpro-2, followed by segregation of the mutant strains and confirmation by PCR. Plasmids pCpcproT-C and pCpcproT-G were then transformed into these strains and unmarked mutants generated by selecting for kanamycin-sensitive, Suc-resistant colonies. The T→C or T→G substitution was confirmed by sequencing of PCR products generated using primers Cpcprointfor and Cpcprointrev. All strains are listed in Supplemental Table S3.

## PBS Purification and Analysis

PBSs were purified according to Glazer (1988). Approximately 100 mL of culture grown to late logarithmic phase was centrifuged at 5,000 rpm, washed twice with 0.8 M potassium phosphate buffer, pH 7 (KP), and resuspended in 1 mL of KP. A total of 500 $\mu$L of 400-$\mu$m beads was added to the cell suspension, and cells were shaken for 10 min using an IKA-VIBRAX-VXR bead beater at 2,400 rpm. The suspension was centrifuged at 13,000 rpm for 20 min, and the supernatant was removed. This was added to a Suc gradient consisting of, from the bottom upward: 1 mL of 2 M, 3 mL of 1 M, 2.5 mL of 0.75 M, 2.5 mL of 0. 5 M, and 2 ml of 0.25 M Suc solutions in KP. The suspension was centrifuged for 20 h at 28,000 rpm. Blue bands containing intact PBSs or free phycobiliproteins were extracted from the Suc gradient. Suc was removed, and samples were concentrated by repeated washing with KP in Amicon Ultra 10K membrane centrifugal filter units.

Samples equivalent to O.D. (620 nm) = 0.2 were analyzed by SDS-PAGE on a Bio-Rad Ready Tris-HCl, 10% to 20% linear polyacrylamide gradient gel in modified Tris/Gly buffer. Gels were run for 20 h at 20 V and then stained with 1% (v/v) Coomassie Blue in acetic acid/methanol. All steps were carried out at room temperature. Identification of PBS proteins was performed by comparison with past studies (Ughy and Ajlani, 2004).

## Absorbance Measurements

Absorbance of all strains was measured according to Merzlyak and Naqvi (2000). Cultures were harvested during the exponential growth phase with an O.D. of 0.6 measured using a spectrophotometer at 750 nm. Cultures were placed in a 4-mL fluorescence cuvette (1 cm path length) and positioned in front of the entrance port of an integrating sphere. A light source sent light via an input fiber into the cuvette containing the sample, and the light leaving the sample in the forward direction was collected by the integrating sphere. The extinction spectra were recorded using a USB4000-UV-VIS Ocean Optics Spectrometer connected to the integrating sphere with an output fiber optic and interfaced to a computer. The cuvettes containing the samples were positioned at different distances (0 and 5 mm) from the entrance port of the sphere, and the absorbance spectrum was obtained via the SpectraSuite Spectroscopy operating software. The nominal absorption spectrum was then calculated using the equation according to Merzlyak and Naqvi (2000).

## Photosynthesis, Photoinhibition, and Respiration Measurements

Photosynthetic oxygen evolution rates and oxygen depletion rates (respiration) were determined on cell cultures (approximately 4 nmol chlorophyll $mL^{-1}$) using an oxygen electrode system (Rank Brothers Instruments) maintained at 30°C. Following dark equilibration (10 min), oxygen-exchange rates were recorded for 10 min at increasing light intensities (10, 25, 60, 150, 350, 900, and 2,000 $\mu$mol photons $m^{-2}$ $s^{-1}$) using MR16 white LED lamps (Deltech). Each light period was followed immediately by 10 min in darkness to calculate the respiration rates. The respiration rate following illumination at each light intensity was subtracted to estimate the real rate of photosynthetic oxygen evolution. To measure photoinhibition, cell cultures (approximately 1 nmol chlorophyll $mL^{-1}$) were first dark equilibrated (10 min), and the rate of oxygen evolution was recorded for 80 min at a light intensity of 2,000 $\mu$E $m^{-2}$ $s^{-1}$. All measurements were standardized to the initial rate. Photoinhibition experiments were conducted either in the absence or presence of lincomycin (250 $\mu$g $mL^{-1}$). A Student's paired $t$ test was used for all comparisons, $P < 0.05$ being considered statistically significant.

## Cell Size

Numbers of cells per unit of volume were measured by counting the cells directly using a Beckman Coulter 2Z particle counter. Measurements were performed using 20 $\mu$L of O.D. (750 nm) = 0.5 cells diluted in 10 mL of measuring buffer. Cell diameter was directly measured using the same instrument. Cell volume was calculated from these measurements. The amount of chlorophyll was measured by subtracting the 750-nm O.D. value from the 680-nm O.D. value and multiplying by 10.854, as described previously (Bombelli et al., 2011; Lea-Smith et al., 2013).

## Light Penetration Measurements

Light penetration was measured using a custom-made apparatus (Supplemental Fig. S8). Light (white LED) was shone from the bottom of the apparatus through the transparent Perspex into the internal chamber. The LED light spectra were measured using an Ocean Optics Spectrometer USB2000+UV-VIS detector (Supplemental Fig. S7). A quantum sensor (Skye Instruments), which measures photosynthetically active radiation uniformly between 400 and 700 nm, was placed on the top of the internal chamber and shone on the top of the cell suspension, to measure light levels. The internal chamber was filled with cells and adjusted to measure light penetration at different depths. Light penetration with red, blue, and green light (Supplemental Fig. S8) at an intensity of 1,000 $\mu$mol photons $m^{-2}$ $s^{-1}$ was performed by using a custom-made light emission device fitted with a LZC-00MC40 RGB LED light (LedEngin).

## Characterization of Mutant Growth

All strains were inoculated using cultures grown under moderate light to late logarithmic phase and then cultured either in conical flasks under continuous light (40 or 150 $\mu$mol photons $m^{-2}$ $s^{-1}$) and shaking or in 250-mL cylindrical plastic containers under continuous light (500 or 1,000 $\mu$mol photons $m^{-2}$ $s^{-1}$) with either air or 5% $CO_2$ bubbling and no shaking. All experiments were conducted in an Infors LED photobioreactor. Absorbance was measured at 625, 652, 680, and 750 nm, to quantify chlorophyll, cell density, and the ratio of APC to PC. Chlorophyll amounts were divided by the 750-nm O.D. value to give a level of chlorophyll per cell in arbitrary units. The ratio of APC to PC was determined by dividing the 652-nm O.D. value by the 625-nm O.D. value. To measure dry cell weights, a volume of culture was removed at the start and end of each growth phase, washed once with distilled water, filtered, and dried prior to measurement. A Student's paired $t$ test was used for all comparisons, $P < 0.05$ being considered statistically significant.

## Bioinformatics

FASTA BLAST comparisons (Altschul et al., 1990) were performed using the *Synechocystis* sp. PCC 6803 *apcE*, *cpcG1*, *cpcC1*, and *cpcC2* sequences against the 86 genomes listed in the National Center for Biotechnology Information database (http://www.ncbi.nlm.nih.gov/sutils/genom_table.cgi).

## Supplemental Data

The following materials are available in the online version of this article.

**Supplemental Figure S1.** Generation of mutant strains in *Synechocystis* sp. PCC 6803.

**Supplemental Figure S2.** Absorbance spectrum of strains.

**Supplemental Figure S3.** Sequence of the upstream region near the altered T→C substitution.

**Supplemental Figure S4.** Light penetration of strains at different O.D. (750 nm) cultures and light levels.

**Supplemental Figure S5.** Growth of strains at 40 and 150 $\mu$mol photons $m^{-2}$ $s^{-1}$ in conical flasks with air bubbling.

**Supplemental Figure S6.** Chlorophyll per cell and ratio of APC to PC of strains under different light, bubbling, and culture conditions.

**Supplemental Figure S7.** Spectra of white, blue, green, and red LED lights.

**Supplemental Figure S8.** Custom-made apparatus used for measuring light penetration.

**Supplemental Table S1.** $\mu$ values of PBS-attenuated strains.

**Supplemental Table S2.** Conservation of PBS subunits in cyanobacteria.

**Supplemental Table S3.** Strains used in this study.

**Supplemental Table S4.** Sequences of primers used in this study.

## ACKNOWLEDGMENTS

We thank Robert Bradley, Nic Ross, Ross Dennis, and Derek Bendall (University of Cambridge) and David Parker, Andrew Murphy, and Karina Almeida Lenero (Shell Global Solutions) for useful discussion.

Received February 3, 2014; accepted April 17, 2014; published April 23, 2014.

## LITERATURE CITED


**Ajlani G, Vernotte C** (1998) Construction and characterization of a phycobiliprotein-less mutant of Synechocystis sp. PCC 6803. Plant Mol Biol **37:** 577–580

**Altschul SF, Gish W, Miller W, Myers EW, Lipman DJ** (1990) Basic local alignment search tool. J Mol Biol **215:** 403–410

**Alvey RM, Biswas A, Schluchter WM, Bryant DA** (2011) Effects of modified phycobilin biosynthesis in the cyanobacterium Synechococcus sp. strain PCC 7002. J Bacteriol **193:** 1663–1671

**Arteni AA, Ajlani G, Boekema EJ** (2009) Structural organisation of phycobilisomes from Synechocystis sp. strain PCC6803 and their interaction with the membrane. Biochim Biophys Acta **1787:** 272–279

**Beckmann J, Lehr F, Finazzi G, Hankamer B, Posten C, Wobbe L, Kruse O** (2009) Improvement of light to biomass conversion by de-regulation of light-harvesting protein translation in Chlamydomonas reinhardtii. J Biotechnol **142:** 70–77

**Bernát G, Waschewski N, Rögner M** (2009) Towards efficient hydrogen production: the impact of antenna size and external factors on electron transport dynamics in Synechocystis PCC 6803. Photosynth Res **99:** 205–216

**Bibby TS, Nield J, Barber J** (2001) Iron deficiency induces the formation of an antenna ring around trimeric photosystem I in cyanobacteria. Nature **412:** 743–745

**Blankenship RE, Tiede DM, Barber J, Brudvig GW, Fleming G, Ghirardi M, Gunner MR, Junge W, Kramer DM, Melis A, et al** (2011) Comparing photosynthetic and photovoltaic efficiencies and recognizing the potential for improvement. Science **332:** 805–809

**Boekema EJ, Hifney A, Yakushevska AE, Piotrowski M, Keegstra W, Berry S, Michel KP, Pistorius EK, Kruip J** (2001) A giant chlorophyll-protein complex induced by iron deficiency in cyanobacteria. Nature **412:** 745–748

**Bombelli P, Bradley RW, Scott AM, Philips AJ, McCormick AJ, Cruz SM, Anderson A, Yunus K, Bendall DS, Cameron PJ, et al** (2011) Quantitative analysis of the factors limiting solar power transduction by Synechocystis sp. PCC 6803 in biological photovoltaic devices. Energy & Environmental Science **4:** 4690–4698

**Bradley RW, Bombelli P, Lea-Smith DJ, Howe CJ** (2013) Terminal oxidase mutants of the cyanobacterium Synechocystis sp. PCC 6803 show increased electrogenic activity in biological photo-voltaic systems. Phys Chem Chem Phys **15:** 13611–13618

**Castenholz RW** (1988) Culturing methods for cyanobacteria. Methods Enzymol **167:** 68–93

**Chen M, Blankenship RE** (2011) Expanding the solar spectrum used by photosynthesis. Trends Plant Sci **16:** 427–431

**Collins AM, Liberton M, Jones HD, Garcia OF, Pakrasi HB, Timlin JA** (2012) Photosynthetic pigment localization and thylakoid membrane morphology are altered in *Synechocystis* 6803 phycobilisome mutants. Plant Physiol **158:** 1600–1609

**Dismukes GC, Carrieri D, Bennette N, Ananyev GM, Posewitz MC** (2008) Aquatic phototrophs: efficient alternatives to land-based crops for biofuels. Curr Opin Biotechnol **19:** 235–240

**Ducat DC, Way JC, Silver PA** (2011) Engineering cyanobacteria to generate high-value products. Trends Biotechnol **29:** 95–103

**Glazer AN** (1988) Phycobilisomes. Methods Enzymol **167:** 304–312

**Glazer AN** (1989) Light guides: directional energy transfer in a photosynthetic antenna. J Biol Chem **264:** 1–4

**Imashimizu M, Fujiwara S, Tanigawa R, Tanaka K, Hirokawa T, Nakajima Y, Higo J, Tsuzuki M** (2003) Thymine at −5 is crucial for cpc promoter activity of Synechocystis sp. strain PCC 6714. J Bacteriol **185:** 6477–6480

**Kaneko T, Sato S, Kotani H, Tanaka A, Asamizu E, Nakamura Y, Miyajima N, Hirosawa M, Sugiura M, Sasamoto S, et al** (1996) Sequence analysis of the genome of the unicellular cyanobacterium Synechocystis sp. strain PCC6803. II. Sequence determination of the entire genome and assignment of potential protein-coding regions (supplement). DNA Res **3:** 185–209

**Kondo K, Ochiai Y, Katayama M, Ikeuchi M** (2007) The membrane-associated CpcG2-phycobilisome in *Synechocystis*: a new photosystem I antenna. Plant Physiol **144:** 1200–1210

**Kwon JH, Bernat G, Wagner H, Rogner M, Rexroth S** (2013) Reduced light-harvesting antenna: consequences on cyanobacterial metabolism and photosynthetic productivity. J Algal Res **2:** 188–195

**Lea-Smith DJ, Ross N, Zori M, Bendall DS, Dennis JS, Scott SA, Smith AG, Howe CJ** (2013) Thylakoid terminal oxidases are essential for the cyanobacterium *Synechocystis* sp. PCC 6803 to survive rapidly changing light intensities. Plant Physiol **162:** 484–495

**McCormick AJ, Bombelli P, Lea-Smith DJ, Bradley RW, Scott AM, Fisher AC, Smith AG, Howe CJ** (2013) Hydrogen production through oxygenic photosynthesis using the cyanobacterium Synechocystis sp PCC 6803 in a bio-photoelectrolysis cell (BPE) system. Energy & Environmental Science **6:** 2682–2690

**Melis A** (2009) Solar energy conversion efficiencies in photosynthesis: minimizing the chlorophyll antennae to maximize efficiency. Plant Sci **177:** 272–280

**Merzlyak MN, Naqvi KR** (2000) On recording the true absorption spectrum and the scattering spectrum of a turbid sample: application to cell suspensions of the cyanobacterium Anabaena variabilis. J Photochem Photobiol B **58:** 123–129

**Mullineaux CW, Tobin MJ, Jones GR** (1997) Mobility of photosynthetic complexes in thylakoid membranes. Nature **390:** 421–424

**Mussgnug JH, Thomas-Hall S, Rupprecht J, Foo A, Klassen V, McDowall A, Schenk PM, Kruse O, Hankamer B** (2007) Engineering photosynthetic light capture: impacts on improved solar energy to biomass conversion. Plant Biotechnol J **5:** 802–814

**Nakajima Y, Tsuzuki M, Ueda R** (1998) Reduced photoinhibition of a phycocyanin-deficient mutant of Synechocystis PCC 6714. J Appl Phycol **10:** 447–452

**Nakajima Y, Ueda R** (1997) Improvement of photosynthesis in dense microalgal suspension by reduction of light harvesting pigments. J Appl Phycol **9:** 503–510

**Page LE, Liberton M, Pakrasi HB** (2012) Reduction of photoautotrophic productivity in the cyanobacterium Synechocystis sp. strain PCC 6803 by phycobilisome antenna truncation. Appl Environ Microbiol **78:** 6349–6351

**Partensky F, Hess WR, Vaulot D** (1999) Prochlorococcus, a marine photosynthetic prokaryote of global significance. Microbiol Mol Biol Rev **63:** 106–127

**Plank T, Anderson LK** (1995) Heterologous assembly and rescue of stranded phycocyanin subunits by expression of a foreign cpcBA operon in Synechocystis sp. strain 6803. J Bacteriol **177:** 6804–6809

**Ried JL, Collmer A** (1987) An nptI-sacB-sacR cartridge for constructing directed, unmarked mutations in gram-negative bacteria by marker exchange-eviction mutagenesis. Gene **57:** 239–246

**Ritchie RJ, Larkum AWD** (2012) Modelling photosynthesis in shallow algal production ponds. Photosynthetica **50:** 481–500

**Savir Y, Noor E, Milo R, Tlusty T** (2010) Cross-species analysis traces adaptation of Rubisco toward optimality in a low-dimensional landscape. Proc Natl Acad Sci USA **107:** 3475–3480

**Ting CS, Rocap G, King J, Chisholm SW** (2001) Phycobiliprotein genes of the marine photosynthetic prokaryote Prochlorococcus: evidence for rapid evolution of genetic heterogeneity. Microbiology **147:** 3171–3182

**Ughy B, Ajlani G** (2004) Phycobilisome rod mutants in Synechocystis sp. strain PCC6803. Microbiology **150:** 4147–4156

**Whitney SM, Houtz RL, Alonso H** (2011) Advancing our understanding and capacity to engineer nature's $CO_2$-sequestering enzyme, Rubisco. Plant Physiol **155:** 27–35

**Xu H, Vavilin D, Funk C, Vermaas W** (2004) Multiple deletions of small Cab-like proteins in the cyanobacterium Synechocystis sp. PCC 6803: consequences for pigment biosynthesis and accumulation. J Biol Chem **279:** 27971–27979

**Zehr JP, Bench SR, Carter BJ, Hewson I, Niazi F, Shi T, Tripp HJ, Affourtit JP** (2008) Globally distributed uncultivated oceanic N2-fixing cyanobacteria lack oxygenic photosystem II. Science **322:** 1110–1112